Poly(ADP-ribosyl)ation temporally confines SUMO-dependent ataxin-3 recruitment to control DNA double-strand break repair

Pfeiffer, A.; Herzog, L.K.; Luijsterburg, M.S.; Shah, R.G.; Rother, M.B.; Stoy, H.; ... ; Dantuma, N.P.

© 2021. Published by The Company of Biologists Ltd | Journal of Cell Science (2021) 134, jcs247809. doi:10.1242/jcs.247809

RESEARCH ARTICLE

Poly(ADP-ribosyl)ation temporally confines SUMO-dependent ataxin-3 recruitment to control DNA double-strand break repair

Annika Pfeiffer[1], Laura K. Herzog[1], Martijn S. Luijsterburg[2], Rashmi G. Shah[3], Magdalena B. Rother[2], Henriette Stoy[1], Ulrike Kühbacher[1], Haico van Attikum[2], Girish M. Shah[3] and Nico P. Dantuma[1,*]

ABSTRACT

DNA damage-induced SUMOylation serves as a signal for two antagonizing proteins that both stimulate repair of DNA double-strand breaks (DSBs). Here, we demonstrate that the SUMO-dependent recruitment of the deubiquitylating enzyme ataxin-3 to DSBs, unlike recruitment of the ubiquitin ligase RNF4, additionally depends on poly [ADP-ribose] polymerase 1 (PARP1)-mediated poly(ADP-ribosyl)ation (PARylation). The co-dependence of ataxin-3 recruitment on PARylation and SUMOylation temporally confines ataxin-3 to DSBs immediately after occurrence of DNA damage. We propose that this mechanism ensures that ataxin-3 prevents the premature removal of DNA repair proteins only during the early phase of the DSB response and does not interfere with the subsequent timely displacement of DNA repair proteins by RNF4. Thus, our data show that PARylation differentially regulates SUMO-dependent recruitment of ataxin-3 and RNF4 to DSBs, explaining how both proteins can play a stimulatory role at DSBs despite their opposing activities.

KEY WORDS: DNA damage response, Ataxin-3, SUMO, Ubiquitin, PARylation, RNF4

INTRODUCTION

The various molecular mechanisms involved in the cellular response to DNA damage are of paramount importance to maintain genome integrity (Hoeijmakers, 2001). To this end, lesions are recognized by specific sensor proteins that initiate a cascade of events resulting in activation of signaling pathways, which coordinate the cellular response to insults as well as trigger proper measures to facilitate the repair of the DNA damage (Jackson and Bartek, 2009). Recognition of the lesion in the context of its natural chromatin environment is followed by marking of the site of DNA damage, which in turn functions as a hub for the coordinated activation of the cellular response to DNA damage and recruitment of the appropriate repair proteins (Lukas et al., 2011; Jackson and Bartek, 2009). Labeling of sites of DNA damage is a crucial step, connecting their recognition by sensor proteins to the cascade of downstream effects that are collectively referred to as the DNA damage response (DDR).

Post-translational modifications (PTMs) of chromatin and chromatin-associated proteins provide a rapid means to instantly label the lesion and its surroundings. The use of PTMs for the recruitment of proteins allows activation of the cellular response with high temporal and spatial precision, avoiding any delay that would be inherently linked to mechanisms that depend on the synthesis of new proteins. The molecular repertoire of PTMs is intimately linked to the DDR and includes, e.g. phosphorylation, ubiquitylation, SUMOylation and poly(ADP-ribosyl)ation (PARylation) (Dantuma and van Attikum, 2016). PTMs typically recruit proteins, which contain binding domains that specifically interact with these modifications and, thereby, position the proteins in proximity to the DNA damage site. Hence, DNA damage-induced PTMs control the dynamic molecular landscape of DNA repair and signaling proteins at DNA lesions (Polo and Jackson, 2011).

More difficult to explain is the functional significance of PTMs that recruit proteins with seemingly opposing activities to DNA lesions. An example of such a situation is the recruitment of the ubiquitin ligase RNF4 and the deubiquitylating enzyme ataxin-3 (ATXN3), which both localize to DNA double-strand breaks (DSBs) by binding to SUMO modifications induced at damaged chromatin (Pfeiffer et al., 2017). Whereas SUMO-targeted RNF4 stimulates ubiquitin-dependent removal of specific DNA repair proteins (Galanty et al., 2012; Luo et al., 2012; Yin et al., 2012), ataxin-3 counteracts this activity by disassembly of the ubiquitin chains on these substrates, resulting in their retention during DNA damage (Pfeiffer et al., 2017). Another layer of complexity arises from the fact that RNF4 and ataxin-3, despite their opposing activities, both stimulate the repair of DSBs (Galanty et al., 2012; Luo et al., 2012; Pfeiffer et al., 2017). A possible explanation for this conundrum is that ataxin-3-mediated retention of DNA repair proteins is stimulatory during the early phase of the DSB response, whereas, at later time points, removal of these proteins by RNF4 is beneficial for correct completion of the repair of DSBs. This model implies a differential regulation of the activity of ataxin-3 and RNF4 at DNA damage sites – which is hard to reconcile with the fact that recruitment of both proteins is facilitated by DNA damage-induced SUMOylation.

In this study, we investigated this model by evaluating the kinetics of ataxin-3 recruitment to DSBs. We found that enrichment of ataxin-3 at DSBs is transient and dependent not only on SUMOylation but also on DNA damage-induced PARylation. In contrast, RNF4 sequestration did not require PARylation. Thus, although RNF4 and ataxin-3 share their ability to interact with SUMO modifications at DSBs, SUMOylation was required but not sufficient for recruitment of ataxin-3. Our data suggest that the combinatorial action of chromatin-associated SUMOylation and PARylation is crucial for coordination of the DSB response, and explains how suppressive and stimulatory roles of RNF4-mediated chromatin eviction of DNA repair proteins can be temporally regulated through PARylation-dependent recruitment of ataxin-3.

[1]Department of Cell and Molecular Biology, Karolinska Institutet, Biomedicum, Solnavägen 9, 17165 Stockholm, Sweden. [2]Department of Human Genetics, Leiden University Medical Center, Einthovenweg 20, 2333 ZC Leiden, The Netherlands. [3]Laboratory for Skin Cancer Research, CHU-Q: University Hospital Research Centre of Quebec (CHUL site) and Laval University, Quebec City (QC) G1V 4G2, Canada.

*Author for correspondence (nico.dantuma@ki.se)

A.P., 0000-0002-0340-5797; N.P.D., 0000-0002-6090-4170

Handling Editor: John Heath
Received 17 April 2020; Accepted 17 December 2020

Journal of Cell Science (2021) 134, jcs247809. doi:10.1242/jcs.247809

RESULTS

Recruitment of ataxin-3 to DSBs is dependent on DNA damage-induced PARylation

When analyzing the recruitment kinetics of green fluorescent protein (GFP)-tagged ataxin-3 to micro-irradiated cells, we noticed that accumulation of ataxin-3 at sites of DNA damage was instant but also very transient in nature (Fig. 1A,B). Approximately 30 min after inflicting damage, ataxin-3 levels had already returned to basal levels. This pattern is very different from the reported accumulation of SUMO conjugates at DSBs, which lasts for several hours (Galanty et al., 2009), and suggests that additional signals are important for recruitment of ataxin-3.

Interestingly, the transient nature of ataxin-3 recruitment resembles the prompt and short-lived generation of poly(ADP-ribose) (PAR) chains at micro-irradiation-inflicted DSBs (Gatti et al., 2020; Luijsterburg et al., 2016). It is well established that this PTM is involved in the recruitment of DNA repair proteins during the early wave of the DDR (Liu et al., 2017). To investigate a possible role of PARylation in the recruitment of ataxin-3, we micro-irradiated, in the absence or presence of the PARP inhibitor KU0058948, U2OS cells expressing mCherry-tagged ataxin-3 and yellow fluorescent protein (YFP)-tagged ALC1, a chromatin remodeler that is recruited to DNA damage in a PARylation-dependent fashion (Ahel et al., 2009; Pines et al., 2012). We found that PARP inhibition prevents not only sequestration of ALC1 but also has a dramatic effect on ataxin-3 recruitment, suggesting that PARylation plays a role in the recruitment of ataxin-3 (Fig. 1C). Quantitative analysis of GFP-ataxin-3 recruitment confirmed a significant reduction in ataxin-3 levels at sites of laser-inflicted damage in PARP inhibitor-treated cells (Fig. 1D; Fig. S1). Treatment with PDD00017273, an inhibitor of the poly(ADP-ribose) glycohydrolase (PARG), which has been shown to efficiently inhibit the removal of PAR oligomers from DSBs (Gogola et al., 2018), prolonged the residence time of ataxin-3 at sites of DNA damage (Fig. 1E,F). To validate the PAR-dependent recruitment of ataxin-3 to DSBs, we took advantage of a system that allows the introduction of breaks by inducing the expression of an mCherry-LacR-FokI nuclease fusion protein that can be tethered to a LacO array in a controllable fashion (Tang et al., 2013). Tethering of the FokI nuclease resulted in accumulation of GFP-ataxin-3 at the array, where it colocalized with PAR polymers (Fig. 1G). Importantly, sequestration of ataxin-3 at FokI foci was also inhibited in response to treatment with PARP inhibitor, confirming a role of PARylation in ataxin-3 recruitment to DSBs (Fig. 1G,H).

The N-terminal domain of ataxin-3 mediates PARylation-dependent recruitment

Ataxin-3 consists of an N-terminal part containing the catalytic Josephin domain, responsible for its deubiquitylating activity, and a C-terminal part containing three ubiquitin-interacting motifs (UIMs) that facilitate binding of ataxin-3 to ubiquitin conjugates (Fig. 2A). To determine the domain of ataxin-3 responsible for the PARylation-dependent recruitment of ataxin-3, GFP-tagged N-terminal and C-terminal fragments of ataxin-3 were expressed, and their recruitment to DSBs was determined in the absence or presence of PARP inhibitor. Interestingly, the N-terminal fragment mimicked the behavior of the full-length ataxin-3, displaying robust translocation to sites of DNA lesions, which was suppressed in cells treated with PARP inhibitor (Fig. 2B). The C-terminal fragment was also recruited to DSBs but its sequestration was different from full-length ataxin-3, as it was independent of PARylation (Fig. 2B). The PARylation-dependent recruitment of the N-terminal fragment of ataxin-3 was confirmed in response to laser-inflicted damage, as PARP inhibitor significantly reduced the levels of the ataxin-3 N-terminal fragment at sites of DNA damage, similar to our observation for full-length ataxin-3 (Fig. 2C,D). These data show that the N-terminal fragment of ataxin-3, comprising the Josephin domain, is responsible for the PARylation-dependent recruitment of ataxin-3 to DSBs. We, therefore, conclude that recruitment of ataxin-3 to DSBs, in addition to SUMOylation, requires DNA damage-induced PARylation.

PARP1-catalyzed PARylation indirectly stimulates ataxin-3 recruitment

PARP1 is the primary enzyme responsible for DNA damage-induced PARylation (Ray Chaudhuri and Nussenzweig, 2017). Interestingly, we found that ataxin-3 physically interacts with PARP1 (Fig. S2A). This interaction was direct and independent of PARylation, as recombinant ataxin-3 co-immunoprecipitated with purified PARP1 (Fig. S2B). It does, however, not substantially contribute to PARylation-dependent recruitment of ataxin-3 to DSBs, as the catalytically inactive PARP1^{E988K} mutant – which still binds ataxin-3 (Fig. S2A) and efficiently localizes to DSBs – failed to restore recruitment of ataxin-3 to laser-inflicted DNA damage in PARP1-deficient cells (Fig. 3A,B). Moreover, the interaction between ataxin-3 and PARP1 was not enhanced upon introduction of DSBs by bleomycin but appeared to be constitutive in nature, which argues against a role of this interaction in DNA damage-induced recruitment of ataxin-3 (Fig. S2C).

We next investigated whether the PARylation-dependent recruitment can be explained by a direct interaction between ataxin-3 and PAR polymers at DNA lesions, as has been observed for other proteins involved in DNA repair (Gupte et al., 2017). Using a southwestern blotting approach, we were, however, unable to detect binding of free PAR polymers to purified ataxin-3, whereas robust binding to purified PARP1, which functioned as a positive control, was readily observed (Fig. 3C). The lack of detectable PAR binding was not due to the denaturing conditions in this assay, as recombinant ataxin-3 lacked PAR-binding activity even in its native conformation (Fig. 3D).

It has recently been reported that PARylation alters the chromatin state at DSBs (Smith et al., 2018), which made us wonder whether an indirect PAR-mediated mechanism is responsible for the stimulation of the SUMO-dependent recruitment of ataxin-3. We addressed this by generating FokI-induced DSBs for 5 h, allowing PAR-dependent chromatin changes to occur as normal, followed by treatment with PARP inhibitor to suppress the subsequent formation of new PAR chains at DSBs. Treatment with PARP inhibitor after FokI-induced DSBs resulted in the complete loss of PAR signal at sites of DNA damage after 5 min – the earliest time-point tested (Fig. 3E; Fig. S3). However, ataxin-3 recruitment at DSBs was still detectable at that time point, after which its presence gradually reduced to background levels, which were reached after 30 min of PARP inhibitor treatment (Fig. 3E,F). The delay in the disappearance of ataxin-3 from DSBs after the PAR signal had vanished is consistent with our observation that ataxin-3 was not recruited by directly binding to PAR polymers. Instead, our data suggest an indirect model, in which PARylation temporarily makes the chromatin surrounding the DSBs permissible for SUMO-dependent recruitment of ataxin-3.

PARylation functionally separates recruitment of ataxin-3 and RNF4 to DSBs

The N-terminal Josephin domain that is responsible for PARylation-dependent recruitment of ataxin-3 is also crucial for SUMO-dependent sequestration of ataxin-3 at DSBs (Pfeiffer et al., 2017).

Journal of Cell Science (2021) 134, jcs247809. doi:10.1242/jcs.247809

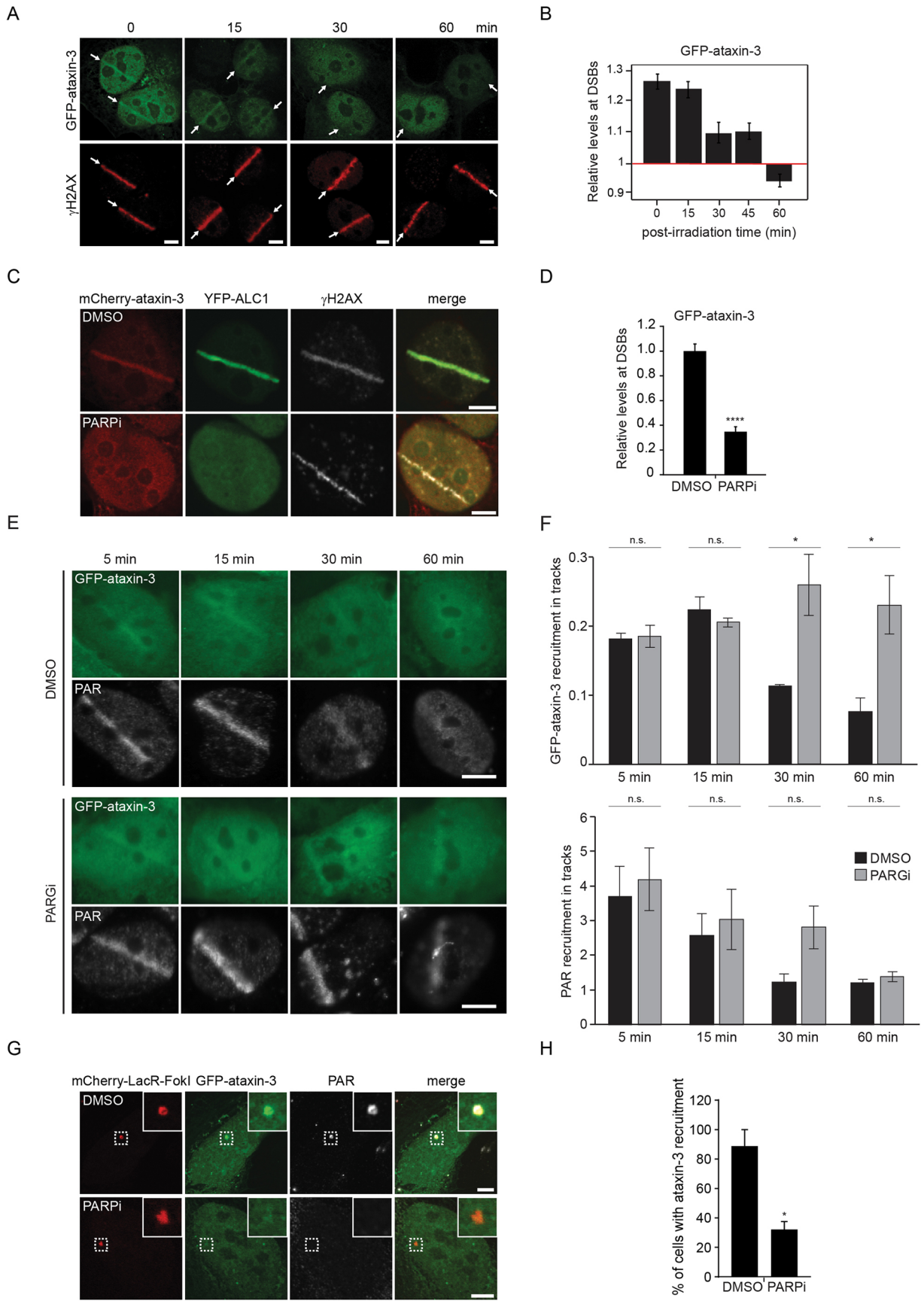

Fig. 1. See next page for legend.

Journal of Cell Science (2021) 134, jcs247809. doi:10.1242/jcs.247809

Fig. 1. Recruitment of ataxin-3 to DSBs is dependent on DNA damage-induced PARylation. (A) U2OS cells transfected with GFP-ataxin-3 were micro-irradiated, fixed at the indicated time points, stained with anti-γH2AX to visualize DSBs, and analyzed using immunofluorescence. Arrows indicate laser tracks. (B) Quantification of the relative fluorescence intensity of GFP-ataxin-3 at DNA damage sites. Note that the levels of ataxin-3 at laser-inflicted damage are expressed as a ratio of the average ataxin-3 intensity in areas of laser damage and the average nuclear ataxin-3 intensity outside the laser-damaged area. Data are presented as mean±s.e.m. with cells pooled from two independent experiments. (C) U2OS cells were transiently transfected with mCherry-ataxin-3 and YFP-ALC1 and treated or not with 10 µM of the PARP inhibitor (PARPi) KU0058948 for 1 h. Cells were micro-irradiated and fixed immediately. Immunolabeling for γH2AX was performed to show DSBs. Merged images are shown on the right. (D) The relative levels of GFP-ataxin-3 at DSBs in the absence or presence of PARPi KU0058948 were quantified. Levels of GFP-ataxin-3 fluorescence in the absence of inhibitor were standardized as 1.0. See Fig. S1. Data are presented as mean±s.e.m. with cells pooled from three independent experiments. ****$P \leq 0.0001$ (Mann–Whitney test). (E) Recruitment of GFP-ataxin-3 to UV-A laser-induced DNA damage tracks 5, 15, 30 and 60 min after DNA damage induction in U2OS cells. Prior to micro-irradiation, cells were treated for 1 h with 10 µM PARG inhibitor (PDD00017273). Cells were then immunostained for PAR to quantify its accumulation. (F) Quantification of GFP-ataxin-3 levels (top graph) and PAR levels (bottom graph) within sites of DNA damage in cells as shown in G. Black bars, DMSO-treated cells; gray bars, PARGi-treated cells, showing the mean ±s.e.m. of three independent experiments. Statistical significance was calculated using the two-tailed Student's *t*-test. n.s., not significant; *$P \leq 0.05$ (G) U2OS FokI DSB reporter cells were transfected with GFP-ataxin-3, incubated with vehicle or 10 µM PARPi KU0058948 for 5 h, while induction of FokI chromatin tethering was simultaneously induced. Cells were then analyzed using immunofluorescence with an anti-PAR antibody. Merged images are shown on the right. Top right of each image shows the magnification of each boxed area. (H) Levels of cells (in %) showing ataxin-3 recruitment to FokI-induced DSBs upon treatment with KU0058948 (PARPi) or upon control treatment (DMSO). Data are presented as mean±s.e.m. from three independent experiments. *$P<0.05$ (unpaired Student's *t*-test). All scale bars: 5 µm.

A plausible explanation for PAR- and SUMO-dependent recruitment of ataxin-3 is that these PTMs occur in a sequential manner at DSBs. To analyze this possibility, we determined whether inhibition of SUMOylation interferes with overall PARylation at DSBs and vice versa. Whereas siRNA-mediated depletion of the SUMO conjugase Ubc9 (officially known as UBE2I), which prevents DNA damage-induced SUMOylation (Galanty et al., 2009), abrogates accumulation of GFP-ataxin-3 at DNA lesions in micro-irradiated cells (Pfeiffer et al., 2017), it did not have a detectable effect on the formation of PAR chains at sites of laser-inflicted damage (Fig. 4A,B). Vice versa, we found that treatment of cells with PARP inhibitor prevented PARylation at DSBs but did not affect accumulation of SUMO1 (Fig. 4C) or SUMO2/3 at DSBs (Fig. 4D). Although this shows that DNA damage-induced PARylation and SUMOylation are largely independent PTMs of DNA damage, it does not exclude the possibility that modifications of specific substrates are interdependent.

Following the observation that DNA damage-induced PARylation and SUMOylation are independent signals, we next asked whether this allows for differential recruitment of ataxin-3 and RNF4 to DSBs. To address this, we analyzed the localization of ataxin-3 and RNF4 at DSBs in mCherry-LacR-FokI-expressing cells in the presence of PARP inhibitor, as we have previously shown that recruitment of these proteins to FokI-induced DSBs strictly depends on SUMOylation (Pfeiffer et al., 2017). Indeed, we found that, whereas PARP inhibitor strongly reduced the accumulation of GFP-ataxin-3 to DSBs, PARP inhibition did not impair translocation of the SUMO-targeted ubiquitin ligase RNF4 to DSBs (Fig. 4E). We, therefore, conclude that DNA damage-induced SUMOylation triggers recruitment of RNF4 independently of PARylation, whereas ataxin-3 requires both PTMs for efficient recruitment.

Ataxin-3 and PARylation promote recruitment of the repair factor XRCC4 to DSBs in an epistatic manner

To address the possibility that PAR-dependent recruitment of ataxin-3 is important for the regulation of the DSB response, we focused on the DNA repair protein XRCC4, since we have previously shown that depletion of ataxin-3 dramatically reduces the steady-state levels of this essential non-homologous end-joining factor at DNA lesions (Pfeiffer et al., 2017). For this purpose, we used U2OS cells that stably express GFP-tagged XRCC4 (GFP-XRCC4) at low levels (Luijsterburg et al., 2016), combined with laser-assisted micro-irradiation followed by live-cell imaging. In agreement with our model, we found that treatment of cells with the PARP inhibitor KU0058948 caused a delay in the recruitment of GFP-XRCC4 to multi-photon laser-inflicted DNA damage (Fig. 5A). Quantitative analysis, furthermore, revealed a dramatic reduction in GFP-XRCC4 sequestration at DNA lesions upon administration of PARP inhibitor (Fig. 5B). To validate these findings and to exclude laser- or PARP inhibitor-specific effects, we used a different PARP inhibitor (olaparib) as well as a UV-A laser to inflict DNA damage. Quantitative analysis showed a very similar reduction in the recruitment of GFP-XRCC4 under these conditions (Fig. 5C; Fig. S4). Importantly, depletion of ataxin-3 did not further reduce GFP-XRCC4 levels at DNA damage sites upon treatment with PARP inhibitor, suggesting that ataxin-3 and PAR polymers are involved in the same mechanism of XRCC4 recruitment (Fig. 5C; Fig. S4). Together, these data are in accordance with our model that PARylation differentiates the recruitment of RNF4 and ataxin-3 to DSBs, thereby regulating translocation of XRCC4 to DNA breaks in order to promote efficient DNA damage repair.

DISCUSSION

The presence of DNA damage induces a broad array of PTMs that decorate chromatin in proximity to the DNA lesions with different spatial and temporal patterns (Bekker-Jensen and Mailand, 2011; Dantuma and van Attikum, 2016; Jackson and Bartek, 2009; Lukas et al., 2011). Our study revealed that localization of ataxin-3 to DSBs is positively regulated by two PTMs – namely SUMO conjugates and PAR polymers, which have to occur simultaneously to facilitate the efficient recruitment of ataxin-3 to sites of DNA damage, while recruitment of RNF4 is dependent on SUMO conjugates but does not require PARylation. We, therefore, propose that the need for both modifications in ataxin-3 recruitment is crucial for the correct functioning of ataxin-3, as this limits the time window during which ataxin-3 is able to prevent RNF4-mediated eviction of DNA repair proteins from chromatin (Fig. 6). For the regulation of the DSB response, it is equally important that binding of SUMO-targeted RNF4 occurs independently of PARylation. This is because the reliance of ataxin-3 recruitment, but not RNF4 recruitment, on both modifications is what allows the differential sequestration of these proteins at DSBs. SUMOylation and PARylation are both versatile signals that are known to be involved in the coordination of the cellular response to various genotoxic insults (Bekker-Jensen and Mailand, 2011; Liu et al., 2017; Ray Chaudhuri and Nussenzweig, 2017). Even though DSBs trigger local enrichment of SUMO and PAR chains, their presence is not limited to sites of DNA damage, as they also regulate gene transcription by changing the composition and condensation of chromatin (Kraus, 2008; Verger et al., 2003). Although PARP1 itself is the predominant target of DNA damage-

Journal of Cell Science (2021) 134, jcs247809. doi:10.1242/jcs.247809

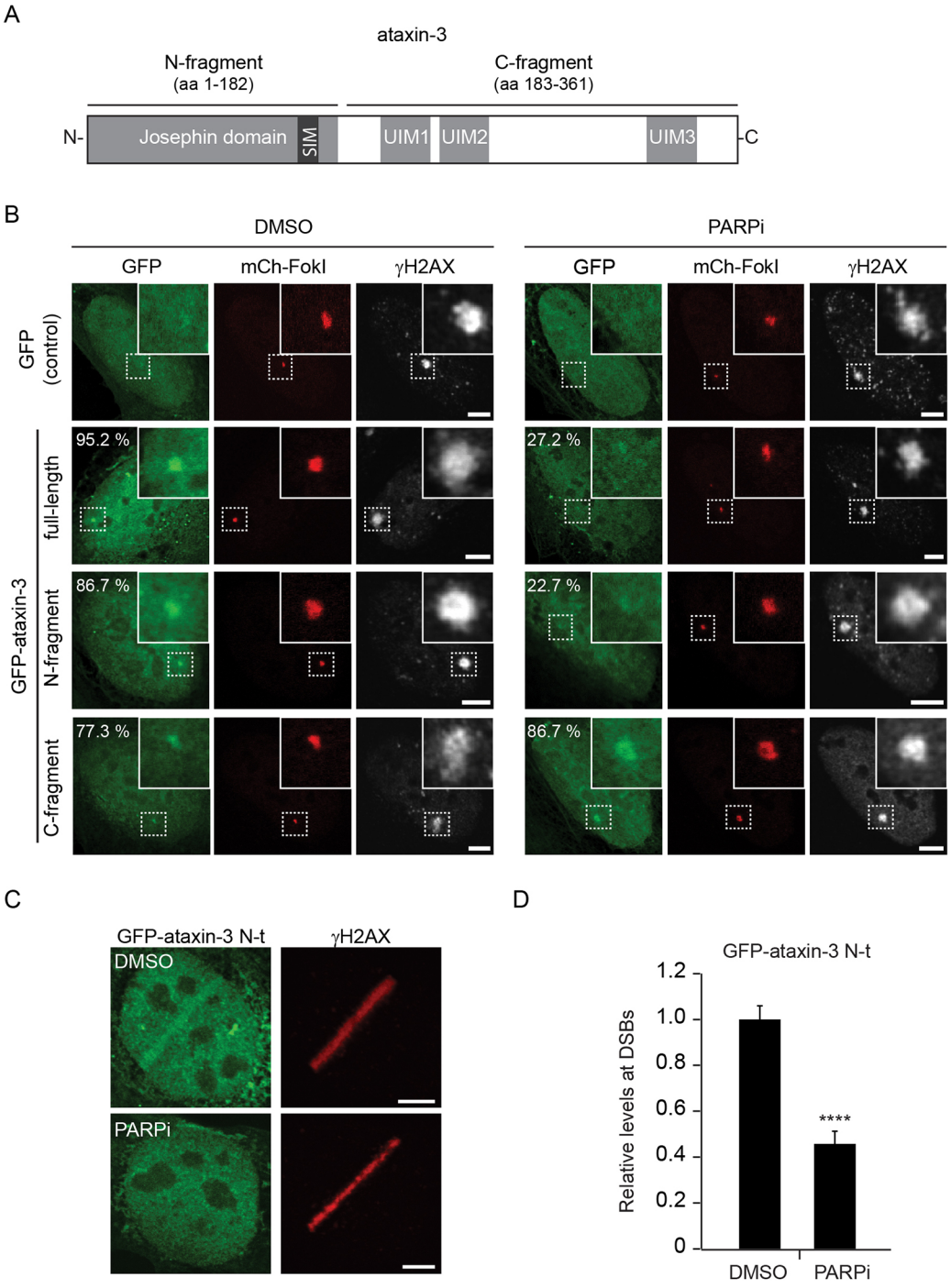

Fig. 2. The N-terminal domain of ataxin-3 mediates PARylation-dependent recruitment. (A) Schematic of full-length ataxin-3. The N-terminal region (amino acids 1–182) constitutes the catalytic Josephin domain and harbors a SUMO-interacting motif (SIM), while the C-terminal region (amino acids 183–361) contains three ubiquitin-interacting motifs (UIM). (B) U2OS FokI DSB reporter cells transfected with GFP (control), GFP-tagged full-length ataxin-3 (full-length), or GFP tagged to the N-terminal or C-terminal regions of ataxin-3 (N-fragment or C-fragment, respectively). All cells were subjected to 1 µM Shield1 and 1 µM 4-OHT for 5 h to induce DSBs, and simultaneously treated with 10 µM of the PARP inhibitor (PARPi) KU0058948 or control treated (DMSO). Immunofluorescence analyses for GFP, mCherry-FokI (mCh-FokI) and γH2AX show the presence of FokI-induced DSBs and recruitment of ataxin-3. The percentage of cells in which the respective GFP-ataxin-3 truncation was recruited to FokI-induced DSBs is indicated in the relevant images; data were derived from at least two independent experiments. Top right of each image shows the magnification of each boxed area (C) U2OS cells transfected with GFP tagged to the N-terminal region of ataxin-3 (GFP-ataxin-3 N-t) were treated with 10 µM KU0058948 (PARPi) or control treated (DMSO) for 1 h prior to micro-irradiation. Cells were fixed immediately after and γH2AX was analyzed by immunofluorescence. (D) Quantification of the relative levels of GFP-ataxin-3 N-t as measured by relative fluorescence intensity at DSBs in cells as shown in C. Data are represented as mean±s.e.m. from three independent experiments. ****$P \leq 0.0001$ (Mann–Whitney test). All scale bars: 5 µm.

induced PARylation (Ray Chaudhuri and Nussenzweig, 2017), SUMO modifications appear to be of a more general nature, resulting in SUMOylation of a broad variety of proteins at DSBs (Bekker-Jensen and Mailand, 2011; Dantuma and Pfeiffer, 2016). It is feasible that the intrinsic action of RNF4 to remove SUMOylated proteins from chromatin prevents inappropriate activation of the DDR. The

Journal of Cell Science (2021) 134, jcs247809. doi:10.1242/jcs.247809

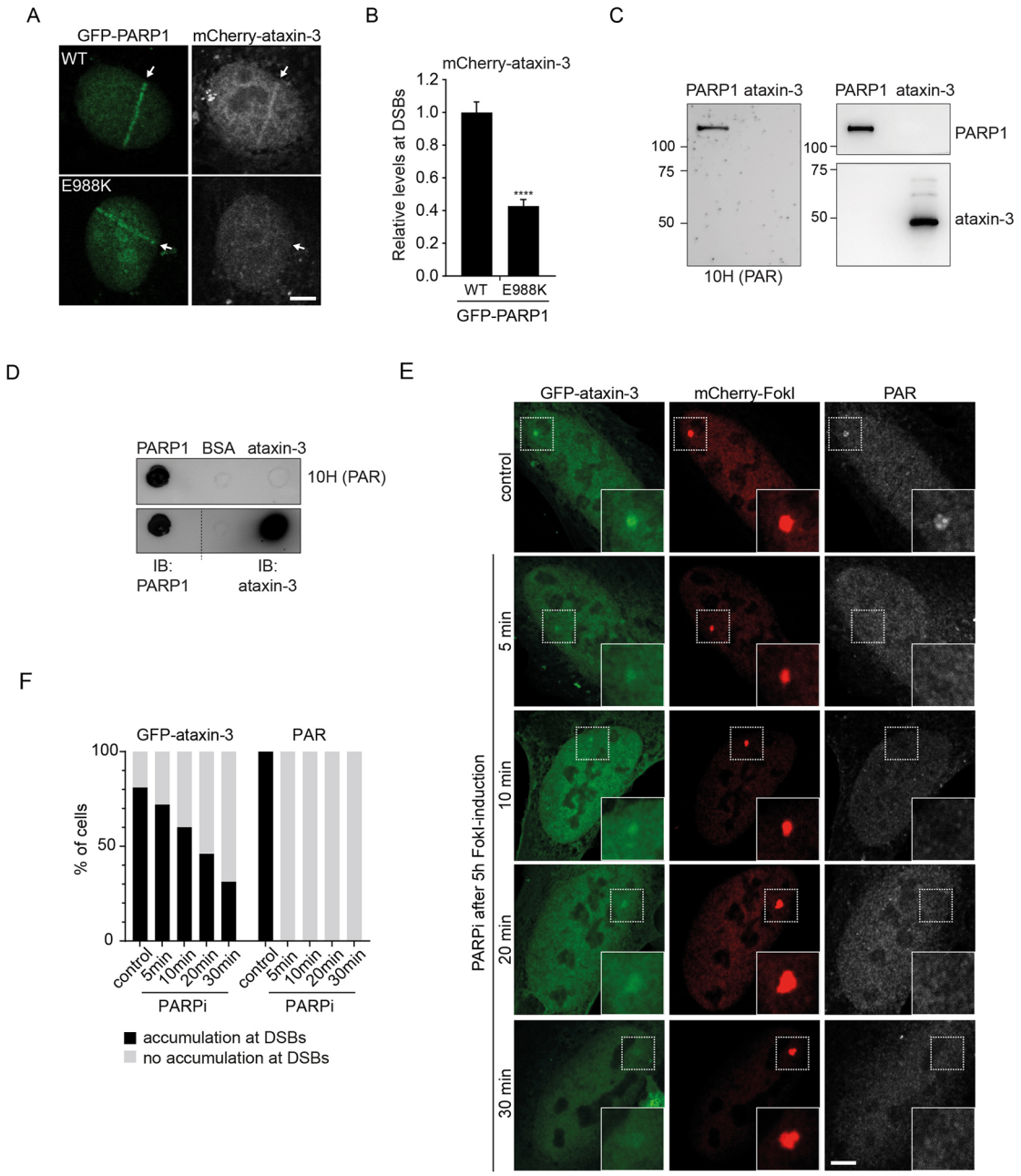

Fig. 3. PARP1-catalyzed PARylation indirectly stimulates ataxin-3 recruitment. (A) PARP$^{-/-}$ U2OS cells were transiently transfected with mCherry-ataxin-3, and wild-type GFP-PARP1 (WT) or mutant GFP-PARP1^{E988K} (E988K), micro-irradiated, immediately fixed and then analyzed by immunofluorescence. (B) Relative fluorescence intensity of mCherry-ataxin-3 at DSBs in cells as shown in A. Data are presented as mean±s.e.m. from three independent experiments. ****$P\leq0.0001$ (Mann–Whitney test). (C) Left: western blot of recombinant human ataxin-3 and PARP separated under denaturing conditions and upon renaturation incubated with PAR chains that were, after stringent washing, detected with anti-PAR antibody (H10 PAR). Right: southwestern blot after probing the membrane with antibodies against ataxin-3 (bottom panel) and PARP1 (top panel), showing that PAR chains bind to PARP1 but not ataxin-3. (D) Dot blots of native recombinant human PARP1, recombinant human ataxin-3 and bovine serum albumin (BSA) spotted on nitrocellulose membrane that was, after incubation with PAR chains and stringent washing, probed with anti-PAR antibody [H10 (PAR)]. Native PARP1 but not ataxin-3 or BSA interacted with PAR chains. Dashed line indicates where membrane was cut. (E) U2OS FokI DSB reporter cells were transfected with GFP-ataxin-3, induced for 5 h with 1 µM Shield1 and 1 µM 4-OHT, followed by treatment with 10 µM of the PARP inhibitor (PARPi) KU0058948 for the indicated periods. Immunofluorescence analysis was performed. Bottom right of each image shows the magnification of each boxed area. (F) Number of cells (in %) in which GFP-ataxin-3 or PAR accumulated at FokI-induced DSBs. Accumulation of GFP-ataxin-3 was scored in a total of 80 cells per condition from two independent experiments. Accumulation of PAR was scored in at least ten cells per condition from two independent experiments. All scale bars: 5 µm.

urgency to control SUMO- and/or ubiquitin-dependent removal of DNA repair proteins is exemplified by another counteracting mechanism that uses the deSUMOylase SENP2, which also regulates DNA damage response by preventing RNF4-mediated extraction (Garvin et al., 2019). The co-occurrence of SUMO conjugates and PAR polymers early in response to DSBs may be a robust mark for newly emerged DSBs, thereby limiting the validating action of ataxin-3 to DSBs.

The use of combinatorial signals in the recruitment of proteins to sites of DNA damage is not unprecedented and has been reported

Journal of Cell Science (2021) 134, jcs247809. doi:10.1242/jcs.247809

for several other proteins involved in DDR (Dantuma and van Attikum, 2016). For example, recruitment of RAP80, a protein that contains SUMO-interacting motifs (SIMs) as well as UIMs, depends on SUMO and ubiquitin chains produced at lesions through the sequential actions of SUMO ligases and RNF4 (Guzzo et al., 2012). Although we have previously found that ataxin-3 binds SUMO (Pfeiffer et al., 2017), it appears that the situation is more complicated when it comes to the role of PARylation in ataxin-3 recruitment, as ataxin-3 does not directly interact with PAR polymers. Instead, the data obtained by us in this study suggest that DNA damage-induced PARylation can indirectly promote the SUMO-dependent recruitment of ataxin-3, similar to what has been reported for CHD4 (Smith et al., 2018) and HP1 (Smith et al., 2019). It has also been shown that PARylation-induced chromatin unfolding promotes the recruitment of DNA-interacting proteins to lesions (Smith et al., 2019), a fact that might have relevance to our data, as ataxin-3 has been shown to interact with DNA (Evert et al., 2006). Therefore PARylation-induced chromatin remodeling might promote ataxin-3 recruitment by exposing SUMO marks at DSBs. Moreover, since RNF4 contains four SIMs (Geoffroy and Hay, 2009) but only a single SIM has been identified in ataxin-3 (Guzzo et al., 2012), RNF4 might bind with higher affinity to SUMO chains, explaining why ataxin-3, but not RNF4, recruitment relies on PARylation.

Recently, it has been reported that ataxin-3 depletion results in hyperaccumulation of the ubiquitin ligase RNF8 at DSBs, which impairs the recruitment of downstream factors and DNA repair (Singh et al., 2019). Although the authors found that depletion of ataxin-3 resulted in significantly reduced recruitment of RNF168 during the first hour after inflicting DNA damage – which is in line with our earlier study (Pfeiffer et al., 2017) – they also observed that this was followed by supraphysiological levels of RNF168 at DSBs (Singh et al., 2019). Since our data suggest that enrichment of ataxin-3 at DSBs only lasts for ∼30 min, we consider the pool of SUMO-targeted ataxin-3 at DSBs unlikely to be involved in the elevated levels of RNF8 several hours after this damage has been inflicted. This does, however, not exclude the possibility that a relatively small population of ataxin-3 – possibly in complex with the segregase valosin-containing protein (VCP) that is involved in the extraction of chromatin-associated proteins (Dantuma and Hoppe, 2012) – facilitates removal of RNF8 from DSBs at late time points. Alternatively, RNF8 hyperaccumulation at DSBs might be an indirect consequence of ataxin-3 activities that take place outside of sites of DNA damage.

We propose two important roles for the PAR/SUMO-dependent regulation of ataxin-3 localization at the DSBs. First, the dependency of DSBs on two PTMs that occur independently of each other at lesions may reduce the risk of inappropriate activation of DDR. Second, the transient nature of the PARylation response, as opposed to the more persistent SUMOylation response, may determine the appropriate time window for ataxin-3 activity at DSBs. Once the PAR signal has ceased to exist and ataxin-3 has left the site of DNA damage, SUMO-recruited RNF4 may stimulate the progression of the DDR by facilitating the timely removal of DNA repair proteins. This model reconciles early studies, which have shown that RNF4-mediated chromatin extraction of DNA repair proteins as well as the counteracting ataxin-3-mediated chromatin retention of these proteins have stimulatory roles in DNA repair (Galanty et al., 2012; Luo et al., 2012; Pfeiffer et al., 2017; Yin et al., 2012).

MATERIALS AND METHODS

Cell culture

Cells were cultured in DMEM GlutaMAX (Thermo Fisher) supplemented with 10% fetal bovine serum (FBS; Thermo Fisher) and 1% penicillin-streptomycin (Thermo Fisher) at 37°C in a humidified incubator with 5% CO_2. Cell lines used in this study were U2OS cells expressing GFP-ataxin-3 (Pfeiffer et al., 2017), U2OS cells expressing GFP-XRCC4 (Luijsterburg et al., 2016), U2OS PARP$^{-/-}$ (Gibbs-Seymour et al., 2016), FokI DSB reporter cells (Tang et al., 2013) and parental U2OS cells. FokI DSB reporter cells stably expressing ER-mCherry-LacR-FokI-DD were induced for 5 h by 1 µM Shield1 (Clontech) and 1 µM 4-OHT (Sigma-Aldrich). Shield protects the ER-mCherry-LacR-FokI-DD fusion from degradation while 4-OHT facilitates its translocation to the nucleus where the FokI nuclease introduces DSBs at an integrated LacO array (Tang et al, 2013). To induce DSBs, the radiomimetic agent bleomycin sulfate (Enzo Life Sciences) was added at 10 µg/ml for 1 h to U2OS cells. For inhibition of PARP, the PARP inhibitors KU0058948 or olaparib (Toronto Research Chemicals) were added, where indicated, at 10 µM for 1 h when DSBs were inflicted by micro-irradiation or 5 h when DSBs were inflicted using the FokI system, to U2OS cells or FokI DSB reporter cells, respectively, unless otherwise stated. For inhibition of PARG, the PARG inhibitor PDD00017273 (Sigma-Aldrich) was used at a final concentration of 10 µM for 1 h prior to micro-irradiation.

Plasmids and RNA interference

The mCherry-ataxin-3 plasmid was generated by exchanging the GFP tag from GFP-ataxin-3 for an mCherry tag by using AgeI/BsrGI restriction sites. Expression plasmids for GFP-ataxin-3, GFP-ataxin-3 N-t, GFP-ataxin-3 C-t, ^{10xHis}ataxin-3^{HA} WT, ^{10xHis}ataxin-3^{HA} C14A (Pfeiffer et al., 2017), EGFP-C1 (Clontech), YFP-ALC1 (gift from Leon Mullenders, Leiden University, The Netherlands), GFP-PARP1 and catalytic inactive GFP-PARP1^{E988K} (gift from Valerie Schreiber, Université de Strasbourg, France) were used. The XRCC4 cDNA (a gift of Penny Jeggo, University of Sussex, UK) was inserted into EGFP-C3-ires-puro (Luijsterburg et al., 2016). Small interfering RNA (siRNA) against *LUC* (siLUC), 5′-CGUACGCGGAAUACUUCGA-3′; *ATX3* (siATX3) #2, 5′-ACGAAGAUGAGGAGGAUUU-3′; Ubc9 (siUbc9), 5′-CAAAAAAUCCCGAUGGCAC-3′ and the AllStars negative control siRNA (siCON) (Qiagen) were used. siRNA oligonucleotides were purchased from GE healthcare/Dharmacon, unless otherwise indicated. Transfections were performed using Lipofectamine 2000 or Lipofectamine RNAiMAX (Thermo Fisher) according to the manufacturer's instructions.

PAR-binding assays

The ability of ataxin-3 to bind free PAR was studied by dot-blot (non-denaturing condition) and southwestern blotting (separation under denaturing conditions followed by renaturation before transfer) as described previously (Robu et al., 2013). The free PAR polymer used in these assays was synthesized by PARP1 activation assay using non-isotopic nicotinamide adenine dinucleotide (NAD) and purified on a dihydroxyboryl boronate (DHBB) column, as described (Shah et al., 2011). For the immune dot blot, PARP1 (1.6 pmol), recombinant ataxin-3 (2.5 pmol), and bovine serum albumin (∼3 pmol) were spotted on a nitrocellulose membrane pre-wetted with TBS-T (10 mM Tris, 150 mM NaCl, 0.05% Tween 20). For southwestern blots, similar quantities of PARP1 and ataxin-3 were resolved on a 10% SDS-PAGE gel. The proteins were renatured by soaking the gel in 20–30 ml of running buffer containing 5% β-mercaptoethanol for 1 h on a rocking platform, at ambient temperature, before transferring them on nitrocellulose. Both the membranes were washed three times with TBS-T and incubated for 1 h at room temperature with 10-15 ml of TBS-T containing 250 nM purified PAR. The membranes were washed three times for 10 min with TBS-T, followed by three washes with TBS-T containing 500 mM NaCl to remove the unbound and loosely bound PAR. The membranes were blocked with TBS-T containing 5% (wt/vol) nonfat milk powder and immunoblotted for PAR using 10H (1:500) antibody purified from culture medium of 10H hybridoma (gift from Dr. M. Miwa, National Cancer Center Research Institute, Tokyo, Japan and Riken Cell Bank). The membranes were stripped with 25 mM glycine, pH 2.0, containing 1% SDS for 15 min at ambient temperature (21°C), and re-probed for PARP1 (rabbit anti-PARP-1, 1:5000, ENZO Life Sciences, catalog no.: ALX-210-302) and ataxin-3 (rabbit anti-ataxin-3, 1:1000, Novus, catalog no.: NBP1-32083) .

Immunofluorescence labeling

Cells were fixed with 4% paraformaldehyde in PBS for 15 min at 4°C. Permeabilization was performed on ice in PBS containing 0.5% Triton

Journal of Cell Science (2021) 134, jcs247809. doi:10.1242/jcs.247809

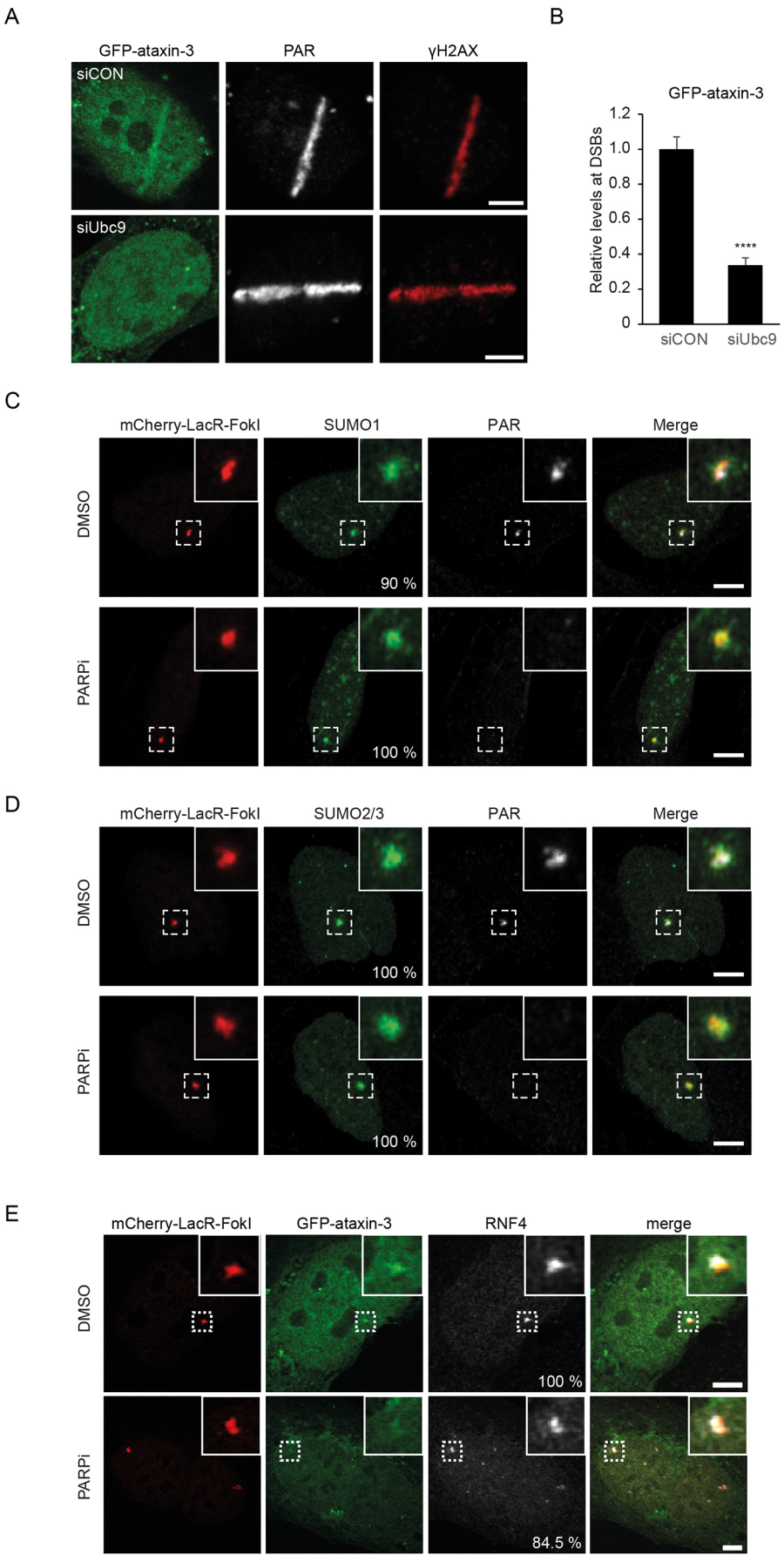

Fig. 4. PARylation functionally separates recruitment of ataxin-3 and RNF4 to DSBs. (A) U2OS cells transfected with GFP-ataxin-3 were treated with control siRNA (siCON) or with siUbc9 to deplete Ubc9, laser micro-irradiated, directly fixed and analyzed by immunofluorescence for ataxin-3, PAR and γH2AX. (B) The relative fluorescence intensity of GFP-ataxin-3 at DSBs in the absence or presence of Ubc9 was quantified. Data were normalized to control and are represented as mean±s.e.m. from three independent experiments. ****$P \leq 0.0001$ (unpaired Student's *t*-test). (C,D) DSB reporter cells induced for 5 h and treated with 10 µM of the PARP inhibitor (PARPi) KU0058948 or with DMSO as control (DMSO). Immunostaining against SUMO1 and PAR (C) and SUMO2/3 and PAR (D) was performed. The percentage of cells in which SUMO1 or SUMO2/3 (C or D, respectively) accumulated at FokI-induced DSBs was scored and is indicated within images. Data shown are derived from two independent experiments. (E) FokI DSB reporter cells were transfected with GFP-ataxin-3 and incubated with vehicle control (DMSO) or 10 µM PARPi KU0058948, simultaneously to induction of FokI chromatin tethering (5 h), followed by immunostaining against RNF4. Percentage of cells in which the RNF4 was recruited to FokI-induced DSBs was scored and is indicated within images. Data shown are derived from two independent experiments. All panels: top right of each image shows the magnification of each boxed area, merged images are shown on the right. All scale bars: 5 µm.

Journal of Cell Science (2021) 134, jcs247809. doi:10.1242/jcs.247809

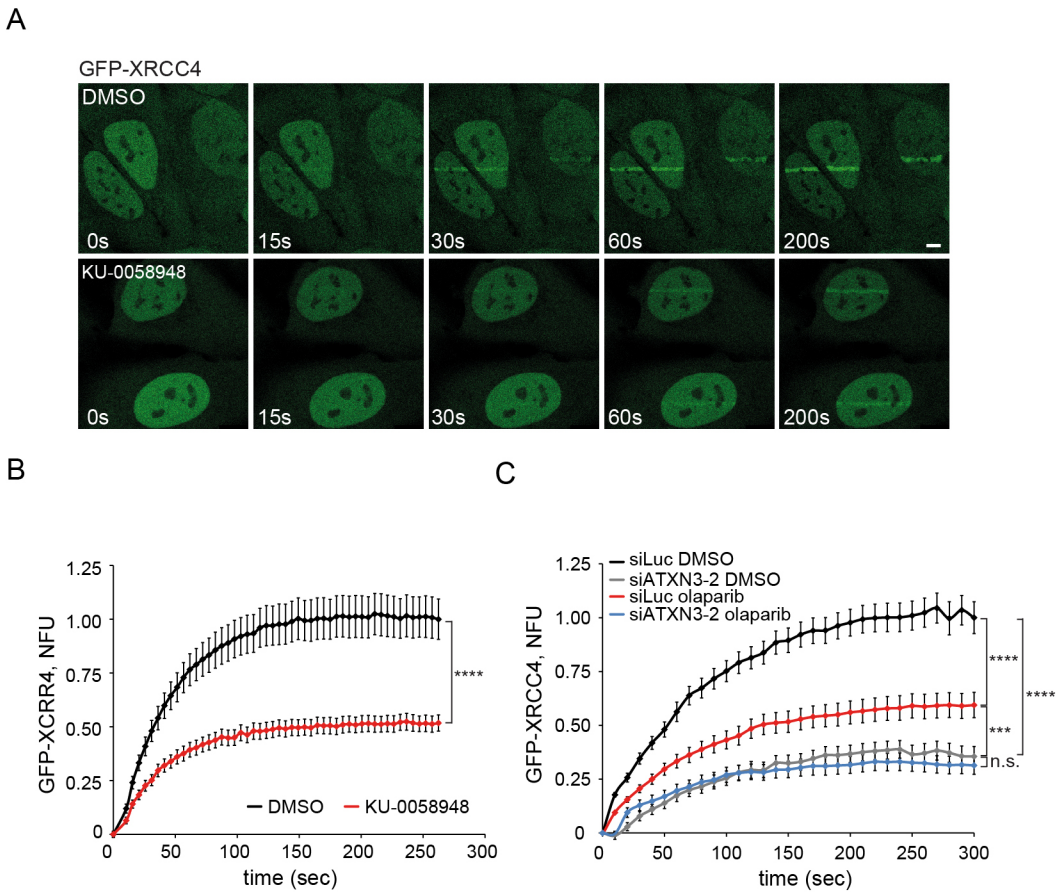

Fig. 5. Ataxin-3 and PARylation promote recruitment of the repair factor XRCC4 to DSBs in an epistatic manner. (A) Stable GFP-XRCC4 cells were treated with DMSO (control) or with 10 µM of the PARP inhibitor KU0058948. Cells were subjected to multiphoton micro-irradiation followed by time-lapse imaging. (B) Quantification of the experiment shown in A. Data represent the average±s.e.m. of 90–100 cells from two independent experiments. Statistical analysis was performed for the last time-point (262 s; unpaired Student's *t*-test). ****$P \leq 0.0001$. (C) Quantification of GFP-XRCC4 recruitment in cells that had been transfected with siRNA against *LUC* or *ATXN3* (siLUC or siATXN3-2, respectively), and treated with DMSO or with 10 µM of the PARP inhibitor olaparib. Cells were sensitized with BrdU and micro-irradiated using a UV-A laser, followed by time-lapse imaging. Data represent the average±s.e.m. of 130–180 cells from two independent experiments. NFU, normalized fluorescence units. Scale bar: 5 µM. Statistical analysis was done for the last time-point (300 s; unpaired Student's *t*-test). n.s., not significant; ***$P \leq 0.001$; ****$P \leq 0.0001$.

X-100 (Sigma-Aldrich) for 5 min followed by quenching with 100 mM glycine (Merck Millipore) for 10 min. Blocking was done in washing buffer WB [PBS supplemented with 0.5% BSA (Sigma-Aldrich) and 0.05% Tween-20 (Sigma-Aldrich)] for 10 min, and primary antibodies were diluted in WB and incubated overnight at 4°C in a humid chamber. Secondary antibodies diluted in WB were incubated at room temperature for 1 h. Staining for DNA with Hoechst dye (Hoechst 33342, Thermo Fisher) in PBS was performed followed by mounting in Mowiol. Primary antibodies and used dilutions were mouse anti-γH2AX (1:1000, Millipore, clone JBW301, catalog no.: MA5-27753), mouse anti-pADPr (10H) (1:200, Santa Cruz, 10H, catalog no.: sc-56198), and rabbit anti-RNF4 (1:500; gift from Jorma Palvimo, University of Eastern Finland, Kuopio, Finland).

Multiphoton laser micro-irradiation

U2OS cells expressing GFP-XRCC4 were grown on 18 mm coverslips and placed in a Chamlide CMB magnetic chamber and the growth medium was replaced by CO_2-independent Leibovitz L15 medium supplemented with 10% FCS and penicillin-streptomycin. PARP inhibitor KU-0058948 was used at 10 µM. Laser micro-irradiation was carried out on a Leica SP5 confocal microscope equipped with an environmental chamber set to 37°C. DSB-containing tracks (1.5 µm width) were generated with a Mira mode-locked titanium-sapphire (Ti:Sapphire) laser (l=800 nm, pulse length=200 fs, repetition rate=76 MHz, output power=80 mW) using a UV-transmitting 63×1.4 NA oil immersion objective (HCX PL APO; Leica). Confocal images were recorded before and after laser irradiation at 5 s or 10 s time intervals over a period of 2–3 min. Images were quantified using Image J.

UV-A laser micro-irradiation

Two methods were used for laser-inflicted DNA damage. The first method has been previously described (Pfeiffer et al., 2017). For the second method, U2OS cells were grown on 18-mm coverslips and sensitized with 10 µM 5′-bromo-2-deoxyuridine (BrdU) for 24 h before micro-irradiation. Cells were transfected with 0.25 µg GFP-ataxin-3 using lipofectamine 2000 (Invitrogen). Cells were pre-treated for 1 h before micro-irradiation with DMSO or PARG inhibitor. For micro-irradiation, cells were placed in a live-cell imaging chamber set to 37°C in CO_2-independent Leibovitz L15 medium supplemented with 10% FCS and penicillin–streptomycin (Invitrogen). Micro-irradiation experiments were carried out with a Zeiss Axio Observer microscope driven by ZEN software using a 63×/1.4 oil immersion objective coupled to a 355 nm pulsed DPSS UV-laser (Rapp OptoElectronic). After micro-irradiation, cells were either used for live cell imaging or fixed at 5, 15, 30 and 60 min with 4% paraformaldehyde and immunostained for PAR chains (Enzo Lifesciences). Images were acquired on a Zeiss AxioImager D2 widefield fluorescence microscope equipped with 63× PLAN APO (1.4 NA) oil-immersion objectives

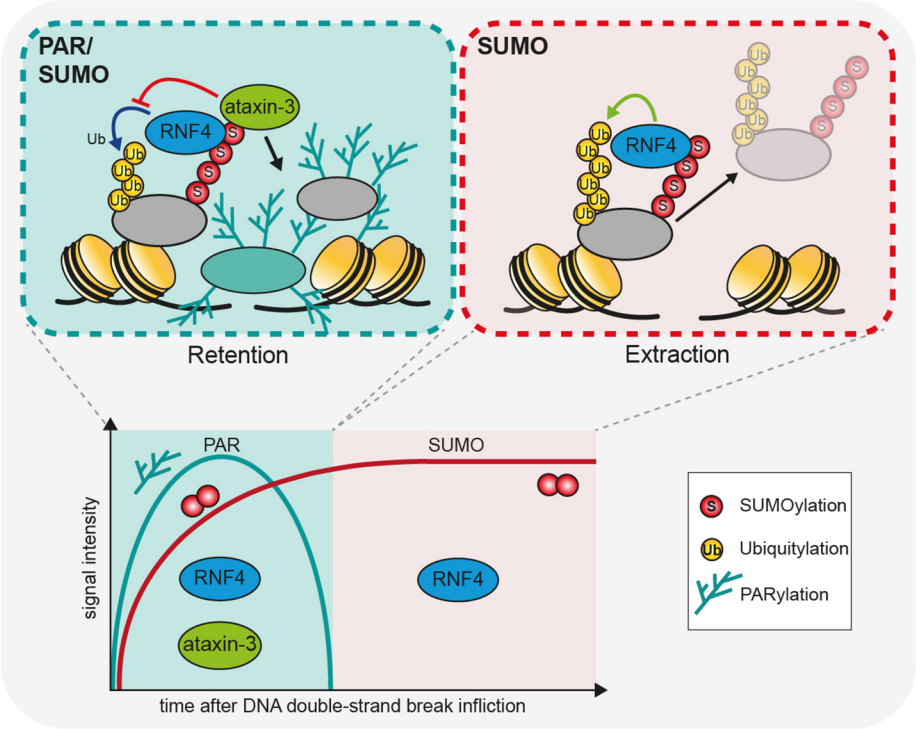

Fig. 6. Model of the differential recruitment of ataxin-3 and RNF4 to DSBs. Recruitment of ataxin-3 to DSBs requires both SUMOylation and PARP1-induced PARylation. This mechanism limits the presence of ataxin-3 to the initial phase of the DSB response, where it prevents premature removal of repair proteins from the newly emerged breaks and promotes efficient activation of the DSB response. Recruitment of RNF4 is only dependent on SUMOylation, a modification that persists for longer than PARylation at DSBs, thereby allowing RNF4 to target its substrates for their timely extraction and to promote efficient repair of DSBs.

(Zeiss), an HXP 120 metal-halide lamp used for excitation. Images were acquired in Zeiss ZEN and quantified in Image J.

Confocal microscopy and image analysis

Images of fixed cells were acquired on a Zeiss LSM510 META confocal microscope equipped with a 63× Plan-A (1.4 NA) oil-immersion lens. Images were recorded using Zeiss LSM imaging software in multi-track mode. Images were analyzed using ImageJ or Zeiss LSM image browser. Quantification of relative protein accumulation at micro-irradiation-induced DSBs was largely done as previously described (Pfeiffer et al., 2017). Additionally, ImageJ was used to measure fluorescence intensity along the damage line and outside the damaged region using line scan (line thickness: 10 pixels) to quantify relative accumulation of proteins at DSBs. The average values are based on the quantification of cells from two or three independent experiments, as indicated in the figure legends. Accumulation of proteins at FokI-induced DSBs was scored manually as the percentage of cells in which the protein-of-interest was found to accumulate at the site. Unless otherwise indicated, 50 cells were counted per condition in two or three independent experiments.

Statistical analysis

Statistical analysis was performed using GraphPad Prism 6.01. To test for a Gaussian data distribution, the Shapiro-Wilk normality test was used. If the normality test was passed, data were analyzed by unpaired Student's *t*-test (two groups) or by one-way Anova test (more than two groups). If the data were not normally distributed, statistical analysis was performed using the nonparametric Mann–Whitney test (two groups) or Kruskal–Wallis test for multiple comparisons. Data are shown as mean from two or three independent experiments. Error bars represent the ±s.e.m. (standard error of the mean). The following *P* values were considered significant $*P \leq 0.05$; $**P \leq 0.01$; $***P \leq 0.001$; $****P \leq 0.0001$.

Acknowledgements

We thank Dr Ivan Ahel (University of Oxford, UK) for the U2OS PARP$^{-/-}$ cells, Dr Julienne O'Rourke (Karolinska Institutet, Stockholm, Sweden) for critical reading of the manuscript and the members of N.P.D.'s group for help and input.

Competing interests

The authors declare no competing or financial interests.

Author contributions

Conceptualization: A.P., M.S.L., H.v.A., G.M.S., N.P.D.; Methodology: A.P., L.K.H., M.S.L., N.P.D.; Validation: A.P., L.K.H., M.S.L., R.G.S., M.B.R., U.K.; Formal analysis: A.P., L.K.H., M.S.L., R.G.S., M.B.R., H.S., U.K., G.M.S., N.P.D.; Investigation: A.P., L.K.H., M.S.L., R.G.S., M.B.R., H.S., U.K.; Data curation: A.P., L.K.H., M.S.L., R.G.S., M.B.R.; Writing - original draft: A.P., N.P.D.; Writing - review & editing: A.P., L.K.H., M.S.L., R.G.S., H.S., U.K., H.v.A., G.M.S., N.P.D.; Visualization: A.P., L.K.H., M.S.L., R.G.S., M.B.R., H.S.; Supervision: A.P., L.K.H., M.S.L., H.v.A., G.M.S., N.P.D.; Project administration: N.P.D.; Funding acquisition: M.S.L., H.v.A., G.M.S., N.P.D.

Funding

This work was supported by a grant from Cancerfonden to N.P.D. (the Swedish Cancer Society, grant no. CAN2018/693), the Vetenskapsrådet to N.P.D. (Swedish Research Council, grant no. 2016-02479), a Nederlandse Organisatie voor Wetenschappelijk Onderzoek (NWO-VIDI) grant to M.S.L. (grant no. 016.161.32), an ERC Consolidator grant to H.v.A. (grant no. ERC-CoG 617485), and the Natural Sciences and Engineering Research Council of Canada (NSERC) Discovery Grant (grant no. RGPIN-2016-05868) and the Discovery Accelerator Supplement Grant (grant no. RGPAS-492875-2016) to G.M.S.

Supplementary information

Supplementary information available online at
https://jcs.biologists.org/lookup/doi/10.1242/jcs.247809.supplemental

Peer review history

The peer review history is available online at
https://jcs.biologists.org/lookup/doi/10.1242/jcs.247809.reviewer-comments.pdf

References

Ahel, D., Horejsi, Z., Wiechens, N., Polo, S. E., Garcia-Wilson, E., Ahel, I., Flynn, H., Skehel, M., West, S. C., Jackson, S. P. et al. (2009). Poly(ADP-ribose)-dependent regulation of DNA repair by the chromatin remodeling enzyme ALC1. *Science* **325**, 1240-1243. doi:10.1126/science.1177321

Bekker-Jensen, S. and Mailand, N. (2011). The ubiquitin- and SUMO-dependent signaling response to DNA double-strand breaks. *FEBS Lett.* **585**, 2914-2919. doi:10.1016/j.febslet.2011.05.056

Dantuma, N. P. and Hoppe, T. (2012). Growing sphere of influence: Cdc48/p97 orchestrates ubiquitin-dependent extraction from chromatin. *Trends Cell Biol.* **22**, 483-491. doi:10.1016/j.tcb.2012.06.003

Dantuma, N. P. and Pfeiffer, A. (2016). Real estate in the DNA damage response: ubiquitin and SUMO ligases home in on DNA double-strand breaks. *Front. Genet.* **7**, 58. doi:10.3389/fgene.2016.00058

Dantuma, N. P. and Van Attikum, H. (2016). Spatiotemporal regulation of posttranslational modifications in the DNA damage response. *EMBO J.* **35**, 6-23. doi:10.15252/embj.201592595

Evert, B. O., Araujo, J., Vieira-Saecker, A. M., de Vos, R. A. I., Harendza, S., Klockgether, T. and Wullner, U. (2006). Ataxin-3 represses transcription via chromatin binding, interaction with histone deacetylase 3, and histone deacetylation. *J. Neurosci.* **26**, 11474-11486. doi:10.1523/JNEUROSCI.2053-06.2006

Galanty, Y., Belotserkovskaya, R., Coates, J., Polo, S., Miller, K. M. and Jackson, S. P. (2009). Mammalian SUMO E3-ligases PIAS1 and PIAS4 promote responses to DNA double-strand breaks. *Nature* **462**, 935-939. doi:10.1038/nature08657

Galanty, Y., Belotserkovskaya, R., Coates, J. and Jackson, S. P. (2012). RNF4, a SUMO-targeted ubiquitin E3 ligase, promotes DNA double-strand break repair. *Genes Dev.* **26**, 1179-1195. doi:10.1101/gad.188284.112

Garvin, A. J., Walker, A. K., Densham, R. M., Chauhan, A. S., Stone, H. R., Mackay, H. L., Jamshad, M., Starowicz, K., Daza-Martin, M., Ronson, G. E. et al. (2019). The deSUMOylase SENP2 coordinates homologous recombination and nonhomologous end joining by independent mechanisms. *Genes Dev.* **33**, 333-347. doi:10.1101/gad.321125.118

Gatti, M., Imhof, R., Huang, Q., Baudis, M. and Altmeyer, M. (2020). The Ubiquitin Ligase TRIP12 limits PARP1 trapping and constrains PARP inhibitor efficiency. *Cell Rep.* **32**, 107985. doi:10.1016/j.celrep.2020.107985

Geoffroy, M.-C. and Hay, R. T. (2009). An additional role for SUMO in ubiquitin-mediated proteolysis. *Nat. Rev. Mol. Cell Biol.* **10**, 564-568. doi:10.1038/nrm2707

Gibbs-Seymour, I., Fontana, P., Rack, J. G. M. and Ahel, I. (2016). HPF1/C4orf27 Is a PARP-1-interacting protein that regulates PARP-1 ADP-Ribosylation activity. *Mol. Cell* **62**, 432-442. doi:10.1016/j.molcel.2016.03.008

Gogola, E., Duarte, A. A., De Ruiter, J. R., Wiegant, W. W., Schmid, J. A., De Bruijn, R., James, D. I., Guerrero Llobet, S., Vis, D. J., Annunziato, S. et al. (2018). Selective loss of PARG restores PARylation and counteracts PARP inhibitor-mediated synthetic lethality. *Cancer Cell* **33**, 1078-1093.e12. doi:10.1016/j.ccell.2018.05.008

Gupte, R., Liu, Z. and Kraus, W. L. (2017). PARPs and ADP-ribosylation: recent advances linking molecular functions to biological outcomes. *Genes Dev.* **31**, 101-126. doi:10.1101/gad.291518.116

Guzzo, C. M., Berndsen, C. E., Zhu, J., Gupta, V., Datta, A., Greenberg, R. A., Wolberger, C. and Matunis, M. J. (2012). RNF4-dependent hybrid SUMO-ubiquitin chains are signals for RAP80 and thereby mediate the recruitment of BRCA1 to sites of DNA damage. *Sci. Signal.* **5**, ra88. doi:10.1126/scisignal.2003485

Hoeijmakers, J. H. J. (2001). Genome maintenance mechanisms for preventing cancer. *Nature* **411**, 366-374. doi:10.1038/35077232

Jackson, S. P. and Bartek, J. (2009). The DNA-damage response in human biology and disease. *Nature* **461**, 1071-1078. doi:10.1038/nature08467

Kraus, W. L. (2008). Transcriptional control by PARP-1: chromatin modulation, enhancer-binding, coregulation, and insulation. *Curr. Opin. Cell Biol.* **20**, 294-302. doi:10.1016/j.ceb.2008.03.006

Liu, C., Vyas, A., Kassab, M. A., Singh, A. K. and Yu, X. (2017). The role of poly ADP-ribosylation in the first wave of DNA damage response. *Nucleic Acids Res.* **45**, 8129-8141. doi:10.1093/nar/gkx565

Luijsterburg, M. S., de Krijger, I., Wiegant, W. W., Shah, R. G., Smeenk, G., de Groot, A. J. L., Pines, A., Vertegaal, A. C. O., Jacobs, J. J. L., Shah, G. M. et al. (2016). PARP1 Links CHD2-mediated chromatin expansion and H3.3 deposition to DNA repair by non-homologous end-joining. *Mol. Cell* **61**, 547-562. doi:10.1016/j.molcel.2016.01.019

Lukas, J., Lukas, C. and Bartek, J. (2011). More than just a focus: the chromatin response to DNA damage and its role in genome integrity maintenance. *Nat. Cell Biol.* **13**, 1161-1169. doi:10.1038/ncb2344

Luo, K., Zhang, H., Wang, L., Yuan, J. and Lou, Z. (2012). Sumoylation of MDC1 is important for proper DNA damage response. *EMBO J.* **31**, 3008-3019. doi:10.1038/emboj.2012.158

Pfeiffer, A., Luijsterburg, M. S., Acs, K., Wiegant, W. W., Helfricht, A., Herzog, L. K., Minoia, M., Böttcher, C., Salomons, F. A., Van Attikum, H. et al. (2017). Ataxin-3 consolidates the MDC1-dependent DNA double-strand break response by counteracting the SUMO-targeted ubiquitin ligase RNF4. *EMBO J.* **36**, 1066-1083. doi:10.15252/embj.201695151

Pines, A., Vrouwe, M. G., Marteijn, J. A., Typas, D., Luijsterburg, M. S., Cansoy, M., Hensbergen, P., Deelder, A., De Groot, A., Matsumoto, S. et al. (2012). PARP1 promotes nucleotide excision repair through DDB2 stabilization and recruitment of ALC1. *J. Cell Biol.* **199**, 235-249. doi:10.1083/jcb.201112132

Polo, S. E. and Jackson, S. P. (2011). Dynamics of DNA damage response proteins at DNA breaks: a focus on protein modifications. *Genes Dev.* **25**, 409-433. doi:10.1101/gad.2021311

Ray Chaudhuri, A. and Nussenzweig, A. (2017). The multifaceted roles of PARP1 in DNA repair and chromatin remodelling. *Nat. Rev. Mol. Cell Biol.* **18**, 610-621. doi:10.1038/nrm.2017.53

Robu, M., Shah, R. G., Petitclerc, N., Brind'Amour, J., Kandan-Kulangara, F. and Shah, G. M. (2013). Role of poly(ADP-ribose) polymerase-1 in the removal of UV-induced DNA lesions by nucleotide excision repair. *Proc. Natl. Acad. Sci. USA* **110**, 1658-1663. doi:10.1073/pnas.1209507110

Shah, G. M., Kandan-Kulangara, F., Montoni, A., Shah, R. G., Brind'Amour, J., Vodenicharov, M. D. and Affar , E. B. (2011). Approaches to detect PARP-1 activation in vivo, in situ, and in vitro. *Methods Mol. Biol.* **780**, 3-34. doi:10.1007/978-1-61779-270-0_1

Singh, A. N., Oehler, J., Torrecilla, I., Kilgas, S., Li, S., Vaz, B., Guérillon, C., Fielden, J., Hernandez-Carralero, E., Cabrera, E. et al. (2019). The p97-Ataxin 3 complex regulates homeostasis of the DNA damage response E3 ubiquitin ligase RNF8. *EMBO J.* **38**, e102361. doi:10.15252/embj.2019102361

Smith, R., Sellou, H., Chapuis, C., Huet, S. and Timinszky, G. (2018). CHD3 and CHD4 recruitment and chromatin remodeling activity at DNA breaks is promoted by early poly(ADP-ribose)-dependent chromatin relaxation. *Nucleic Acids Res.* **46**, 6087-6098. doi:10.1093/nar/gky334

Smith, R., Lebeaupin, T., Juhász, S., Chapuis, C., D'Augustin, O., Dutertre, S., Burkovics, P., Biertümpfel, C., Timinszky, G. and Huet, S. (2019). Poly(ADP-ribose)-dependent chromatin unfolding facilitates the association of DNA-binding proteins with DNA at sites of damage. *Nucleic Acids Res.* **47**, 11250-11267. doi:10.1093/nar/gkz820

Tang, J., Cho, N. W., Cui, G., Manion, E. M., Shanbhag, N. M., Botuyan, M. V., Mer, G. and Greenberg, R. A. (2013). Acetylation limits 53BP1 association with damaged chromatin to promote homologous recombination. *Nat. Struct. Mol. Biol.* **20**, 317-325. doi:10.1038/nsmb.2499

Verger, A., Perdomo, J. and Crossley, M. (2003). Modification with SUMO. A role in transcriptional regulation. *EMBO Rep.* **4**, 137-142. doi:10.1038/sj.embor.embor738

Yin, Y., Seifert, A., Chua, J. S., Maure, J.-F., Golebiowski, F. and Hay, R. T. (2012). SUMO-targeted ubiquitin E3 ligase RNF4 is required for the response of human cells to DNA damage. *Genes Dev.* **26**, 1196-1208. doi:10.1101/gad.189274.112